Article

Cross Surface Ambipolar Charge Percolation in Molecular Triads on Mesoscopic Oxide Films

Qing Wang, Shaik M. Zakeeruddin, Jens Cremer, Peter Buerle, Robin Humphry-Baker, and Michael Grtzel

J. Am. Chem. Soc., **2005**, 127 (15), 5706-5713• DOI: 10.1021/ja0426701 • Publication Date (Web): 25 March 2005

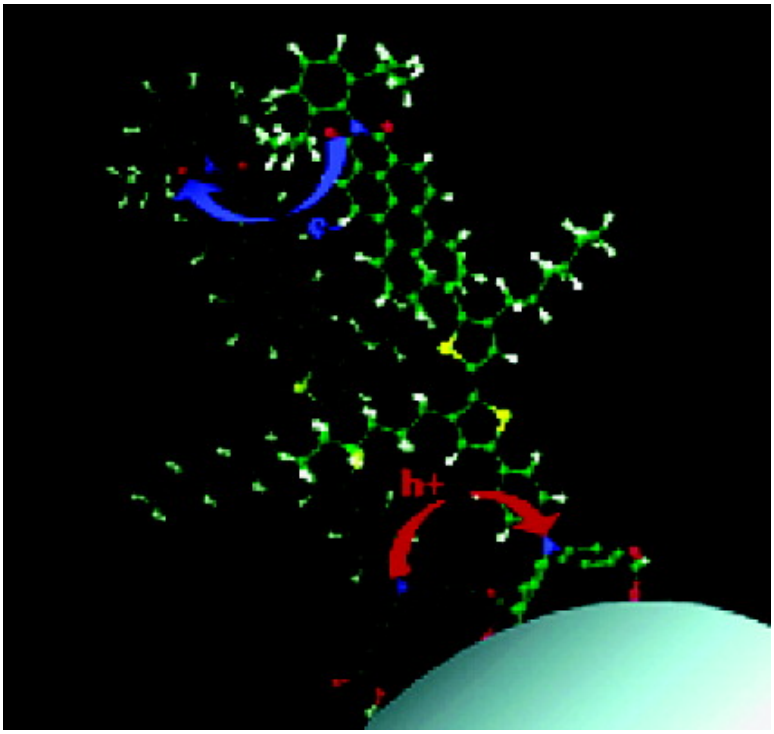

More About This Article

Additional resources and features associated with this article are available within the HTML version:

- Supporting Information
- Links to the 3 articles that cite this article, as of the time of this article download
- Access to high resolution figures
- Links to articles and content related to this article
- Copyright permission to reproduce figures and/or text from this article

J|A|C|S
ARTICLES
Published on Web 03/25/2005

Cross Surface Ambipolar Charge Percolation in Molecular Triads on Mesoscopic Oxide Films

Qing Wang,[†] Shaik M. Zakeeruddin,[†] Jens Cremer,[‡] Peter Bäuerle,[‡] Robin Humphry-Baker,[†] and Michael Grätzel*,[†]

Contribution from the Laboratory for Photonics and Interfaces, Ecole Polytechnique Fédérale, CH-1015 Lausanne, Switzerland, and Department of Organic Chemistry II, University of Ulm, 89081 Ulm, Germany

Received December 6, 2004; E-mail: michael.graetzel@epfl.ch

Abstract: We report on cross surface ambipolar charge percolation within a monolayer of a molecular triad adsorbed on semiconducting or insulating mesoscopic metal oxide films. The triad consists of a triphenlyamine (TPA) donor and a perylenemonoimide (PMI) acceptor connected by a bithiophene (T2) bridge. The self-assembled **PMI-T2-TPA** monolayer exhibits p-type or n-type conduction depending on the potential that is applied to the conducting glass (FTO) electrode supporting the oxide films. Cross surface electron transfer is turned on at around −1.24 V (vs Fc+/Fc) where the PMI moiety is electroactive. The color of the film changes from red to blue during the reduction of the PMI. By contrast, lateral hole transfer is turned on at around 0.8 V (vs Fc+/Fc) where the TPA moiety becomes electroactive. The stepwise oxidation of the T2-TPA units at 0.79 and 1.28 V (vs Fc+/Fc) is associated with a color change of the film from red to black. Cyclic voltammetric as well as chronocoulometric and spectroelectrochemical measurements were applied to determine the percolation threshold for cross surface charge transfer and the diffusion coefficients for the electron and hole hopping process. The effect of oxide surface states on the lateral charge motion was also investigated.

Introduction

Mesoscopic oxide films are under intensive investigation for a variety of optoelectronic applications such as dye-sensitized solar cells, intercalation batteries, and electrochromic and electroluminescent displays, as well as environmental sensors and biosensors.[1−9] A recently discovered intriguing phenomenon is the occurrence of efficient lateral charge motion within a monolayer of a redox relay adsorbed onto the highly corrugated surface of such films. Thus, self-assembled monolayers of triarylamines and fullerene derivatives anchored on insulating films of Al_2O_3, TiO_2, and ZrO_2 exhibit two-dimensional conduction when their surface coverage exceeds the percolation threshold.[10−12]

Triarylamines and thiophenes are widely used as hole conductors in thin layer electro-optical devices such as organic light emitting diodes (OLEDs), solar cells, and organic field-effect transistors (OFETs).[13,14] By contrast, perylenes are known to be excellent electron conductors and are used as n-type organic semiconductors in OFETs[15] and photovoltaic cells, apart from assuming antenna and energy-transfer functions in fluorescent concentrators. The present study reports on the synthesis and ambipolar conduction behavior of the molecular triad **PMI-T2-TPA**. The latter molecule connects a perylenemonoimid moiety (PMI), a typical π-electron acceptor and a triphenylamine unit (TPA) via a bithiophene spacer (T2) both being π-electron donors. The change in redox state of these donor and acceptor moieties is accompanied by a striking and reversible color change.

Electrochromic materials have gained widespread interest for applications in display panels, electrochemical windows, and mirrors. The ability to realize the three complementary colors, red, green, and blue (RGB), constitutes an important step toward the use of molecular electrochromic devices. However, it has been difficult to find molecules exhibiting green electrochromism.[16] Very recently, a successful attempt in this direction was reported showing that an RGB electrochromic device can be constructed from one polymer containing two well-defined,

[†] Ecole Polytechnique Fédérale.
[‡] University of Ulm.

(1) O'Regan, B.; Gräzel, M. *Nature* **1991**, *353*, 737−740.
(2) Grätzel, M. *Nature* **2001**, *414*, 338−344.
(3) Bonhôte, P.; Gogniat, E.; Campus, F.; Walder, L.; Grätzel, M. *Displays* **1999**, *20*, 137−144.
(4) Huang, S. Y.; Kavan, L.; Exnar, I.; Grätzel, M. *J. Electrochem. Soc.* **1995**, *142*, L142-L144.
(5) Gopel, W.; Schierbaum, K. D. *Sens. Actuators, B* **1995**, *26*, 1−12.
(6) Möller, M. T.; Asaftei, S.; Corr, D.; Ryan, M.; Walder, L. *Adv. Mater.* **2004**, *16*, 1558−1562.
(7) Cinnsealach, R.; Boschloo, G.; Rao, S. N.; Fitzmaurice, D. *Sol. Energy Mater. Sol. Cells* **1998**, *55*, 215−223.
(8) Long, B.; Nikitin, K.; Fitzmaurice, D. *J. Am. Chem. Soc.* **2003**, *125*, 5152−5160.
(9) Long, B.; Nikitin, K.; Fitzmaurice, D. *J. Am. Chem. Soc.* **2003**, *125*, 15490−15498.
(10) Bonhôte, P.; Gogniat, E.; Tingry, S.; Barbé, C.; Vlachopoulos, N.; Lenzmann, F.; Comte, P.; Grätzel, M. *J. Phys. Chem. B* **1998**, *102*, 1498−1507.
(11) Papageorgiou, N.; Grätzel, M.; Enger, O.; Bonifazi, D.; Diederich, F. *J. Phys. Chem. B* **2002**, *106*, 3813−3822.
(12) Westermark, K.; Tingry, S.; Persson, P.; Rensmo, H.; Lunell, S.; Hagfeldt, A.; Siegbahn, H. *J. Phys. Chem. B* **2001**, *105*, 7182−7187.
(13) Shirota, Y. *J. Mater. Chem.* **2000**, *10*, 1−25.
(14) Thelakkat, M. *Macromol. Mater. Eng.* **2002**, *287*, 442−461.
(15) Dimitrakopoulos, C. D.; Malenfant, P. R. L. *Adv. Mater.* **2002**, *14*, 99−117.

10.1021/ja0426701 CCC: $30.25

Scheme 1. Synthesis of **PMI-T2-TPA**

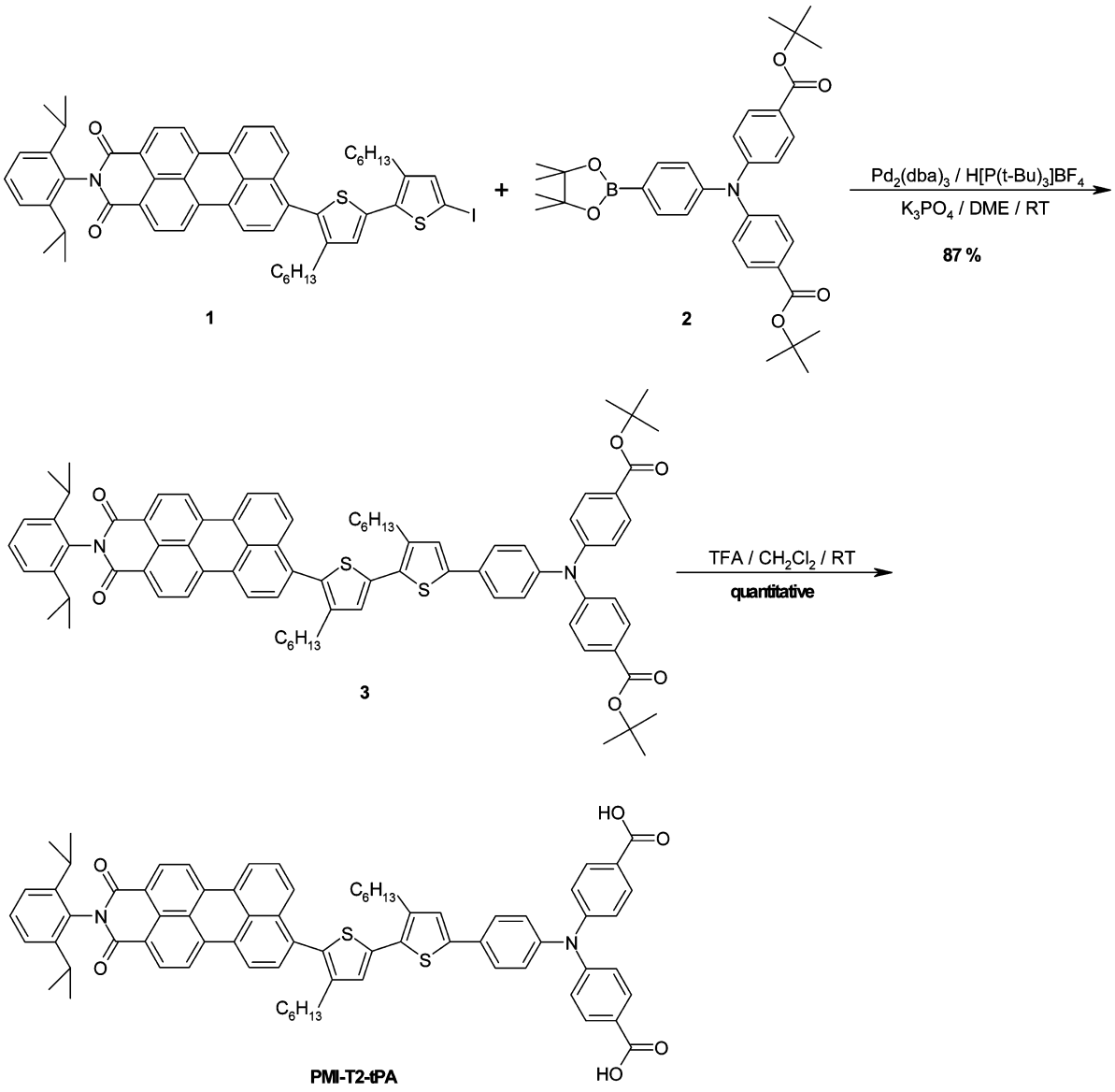

isolated, conjugated systems which absorb blue and red light.[17] The virtue of the system presented in this study is that it would ultimately enable the design of RGB molecular electrochromic devices.

Understanding intra- and intermolecular electronic communication is essential for the rational design and realization of devices functioning on the nanoscale. One preferred approach for the molecules and their connection to the macroscopic world relies on self-organization to form self-assembled monolayers (SAMs).[18,19] The present study deals with the self-assembly of **PMI-T2-TPA** molecules on mesoscopic oxide films and explores the charge transport properties of such monomolecular layers.

Experimental Section

Materials. *n*-Hexadecylmalonic acid (HDMA) and tetra-*n*-butylammonium hexafluorophosphate ($TBAPF_6$) were purchased from Lancaster and Fluka, respectively. 1-Ethyl-3-methylimidazolium bis(trifluoromethanesulfonyl)amide (EMITFSI) was synthesized according to literature procedure.[20]

Synthesis of PMI-T2-TPA. The synthesis of the target molecule **PMI-T2-TPA** is depicted in Scheme 1. The synthesis starts from perylenyl-bithiophene **1** that bears a reactive iodine function at the free α-position of the bithiophene unit. This donor−acceptor molecule is one member of a series of hybrid systems that we recently prepared. Iodide **1** is coupled with triphenylamine boronic ester **2** in a Pd-catalyzed Suzuki-type coupling to yield the triad precursor molecule **3** in 87% yield. The *tert*-butyl-protected ester groups that are attached in the *para*-position of two phenyl units of the triarylamine are saponified by reaction with trifluoroacetic acid to quantitatively yield the diacid **PMI-T2-TPA**. Detailed synthetic procedure and the characterization of molecule are included as the Supporting Information.

Preparation of Mesoscopic Oxide Film. The TiO_2 colloid was prepared using published procedures.[21] A paste consisting of TiO_2 colloid and ethyl cellulose in terpineol was deposited using the "doctor blading" technique on a fluorine-doped SnO_2 conducting glass (TEC15,

(16) Monk, P. M. S.; Mortimer, R. J.; Rosseinsky, D. R. *Electrochromism: Fundamentals and Applications;* Wiley-VCH: Weinheim, 1995.
(17) Sonmez, G.; Shen, C. K. F.; Rubin, Y.; Wudl, F. *Angew. Chem., Int. Ed.* **2004**, *43*, 1498−1502.
(18) Bard, A. J. *Integrated Chemical Systems: A Chemical Approach to Nanotechnology;* John Wiley & Sons: New York, 1994.
(19) Finklea, H. O. *Electroanalytical Chemistry;* Marcel Dekker: New York, 1996; pp 110−335.
(20) Bonhôte, P.; Dias, A. P.; Papageorgiou, N.; Kalyanasundaram, K.; Grätzel, M. *Inorg. Chem.* **1996**, *35*, 1168−1178.

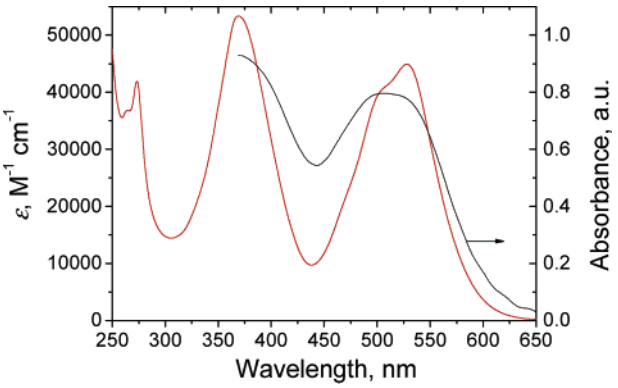

Figure 1. UV−vis spectrum of **PMI-T2-TPA** ($c = 5 \times 10^{-5}$ M) in dichloromethane (red line) and on mesoscopic TiO_2 film (black line).

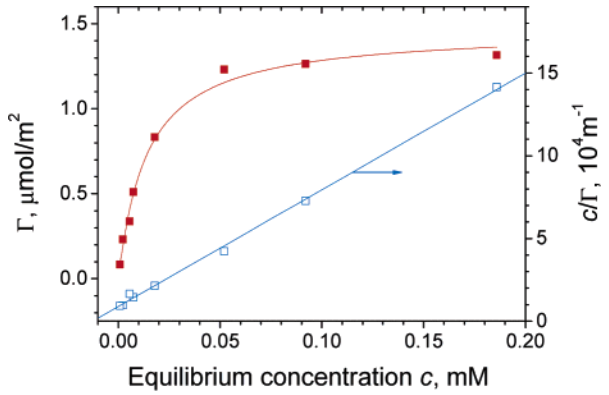

Figure 2. Adsorption isotherm of **PMI-T2-TPA** on mesoscopic TiO_2 film from acetone solutions. The square dots are measured points, and the line is the fit with a Langmuir equation. The right axis is its linearized plot.

15Ω/Sq.) to form a transparent layer. Subsequently, the deposited film was heated to 500 °C in an oxygen atmosphere and calcinated for 10 min. The final film thickness was determined by using an Alpha-step 200 surface profilometer (Tencor Instruments, USA) to be ca. 6 μm. A porosity of 0.63 and roughness factor of ~660 for the transparent layer were measured with a Gemini 2327 nitrogen adsorption apparatus (Micromeretics Instrument Corp., USA). The nanocrystalline Al_2O_3 film was prepared as described in ref 10. The nanocrystalline metal oxide films were first sintered at 500 °C for 20 min in air and after cooling to 80 °C immersed in a solution of 0.30 mM **PMI-T2-TPA** in acetone for 3 h to produce **PMI-T2-TPA** derivatized films.

UV−vis and ATR-FTIR Measurements. UV−vis spectra were measured on a Cary 5 spectrophotometer. ATR-FTIR analysis employed a FTS700 FTIR spectrometer (Digilab, USA). Samples were measured under a mechanical force pushing the film in contact with the diamond window. Spectra were derived from 64 scans at a resolution of 2 cm^{-1}. Prior to measuring the spectra, the **PMI-T2-TPA** derivatized films were rinsed in acetonitrile to wash out any weakly adsorbed molecules and dried.

Electrochemical Measurements. Voltammetric and chronocoulometric measurements employed a PC-controlled AutoLab PSTAT10 electrochemical workstation (Eco Chimie). Cyclic voltammograms (CV) were obtained at a scan rate of 0.02 V/s using the ionic liquid 1-ethyl-3-methylimidazolium bis(trifluoromethanesulfonyl)imide (EMITFSI) as electrolyte and the mesoscopic metal oxide film as working electrode. Chronocoulometric measurements were carried out under the same conditions. Cyclic voltammetry was also performed with 1 mM **PMI-T2-TPA** in dichloromethane containing 0.1 M $TBAPF_6$ supporting electrolyte to examine the electrochemical behavior of the triad on a platinum disk electrode (2 mm in diameter). In all cases a platinum coil and $Ag/AgNO_3$ electrode were employed as the counter and reference electrode, respectively. Unless otherwise noted, the potentials reported below use the ferrocene/ferrocinium (Fc+/Fc) couple as an internal reference.

Results

UV−vis Absorption and ATR-FTIR Spectra of PMI-T2-TPA. PMI-T2-TPA consists of perylenemonoimid and triphenylamine units connected by a bithiophene bridge, Scheme 1. The two carboxylate groups attached to the arylamine afford strong anchoring on the oxide surface. The UV/vis absorption spectrum measured in dichloromethane solution exhibits three main absorption bands at $\lambda_1 = 273$ nm, $\lambda_2 = 528$ nm, and $\lambda_3 = 369$ nm (Figure 1). The first two transitions can be assigned to the perylene unit, whereas the last results from the TPA-T2 moiety, the two chromophores being in full conjugation. This is corroborated by the absorption spectrum of the independently synthesized subunit PMI-T2 dyad where the perylene bands are maintained at $\lambda_1 = 261$ nm and $\lambda_2 = 517$ nm while the bithiophene maximum is blue shifted to $\lambda_3 = 300$ nm. In comparison, the adsorption of **PMI-T2-TPA** on mesoscopic TiO_2 film shows a quite broad absorption peak at around 510 nm.

The adsorption isotherm of **PMI-T2-TPA** on mesoscopic TiO_2 films was obtained by equilibrating the electrodes with different concentrations of **PMI-T2-TPA** in acetone and measuring the concentration change (Δc) of the solutions. The surface concentrations Γ were obtained from eq 1:

$$\Gamma = \frac{V\Delta c}{\eta S} \tag{1}$$

where V is the volume of solution, η is the roughness factor, and S is the apparent area of electrodes. The experimental values fit the Langmuir adsorption isotherm (Figure 2)

$$\Gamma = \frac{\Gamma_0 c}{\left(c + \frac{1}{K}\right)} \tag{2}$$

where c is the concentration of **PMI-T2-TPA** solution in acetone, Γ_0 is the surface concentration at full monolayer coverage, and K is the adsorption constant. The best fit was obtained with $\Gamma_0 = 1.46 \pm 0.05$ μmol/m^2 and $K = 71.5 \pm 8.3$ mM^{-1}, which corresponds to an area of 1.14 nm^2 per molecule. Given the molecular diameter of 1.06 nm determined by molecular modeling, it is consistent with a monolayer adsorption of **PMI-T2-TPA** on the TiO_2 surface. Presumably, because of the bulky structure of **PMI-T2-TPA**, Γ_0 is almost 2 times lower than that of the phosphonated triarylamine.[10]

Figure 3 compares the FTIR spectrum of a **PMI-T2-TPA** powder with that of the monolayer adsorbed on a mesoscopic TiO_2 film. The IR spectra are similar in the pure and adsorbed state. Vibrations from C=C ring stretching at 1574, 1593, the imide C=O at 1668, 1709 cm^{-1}, and C−N stretching at 1267 cm^{-1} are clearly seen in the spectra for both samples.[22−25]

(21) Barbé, C. J.; Arendse, F.; Comte, P.; Jirousek, M.; Lenzmann, F.; Shklover, V.; Grätzel, M. *J. Am. Ceram. Soc.* **1997**, *80*, 3157−3171.

(22) Rodriguez-Llorente, S.; Aroca, R.; Duff, J. *Spectrochim. Acta, Part A* **1999**, *55*, 969−978.

(23) Kvarnström, C.; Petr, A.; Damlin, P.; Lindfors, T.; Ivaska, A.; Dunsch, L. *J. Solid State Electrochem.* **2002**, *6*, 505−512.

(24) Del Caño, T.; Duff, J.; Aroca, R. *Appl. Spectrosc.* **2002**, *56*, 744−750.

(25) Reva, I.; Lapinski, L.; Chattopadhyay, N.; Fausto, R. *Phys. Chem. Chem. Phys.* **2003**, *5*, 3844−3850.

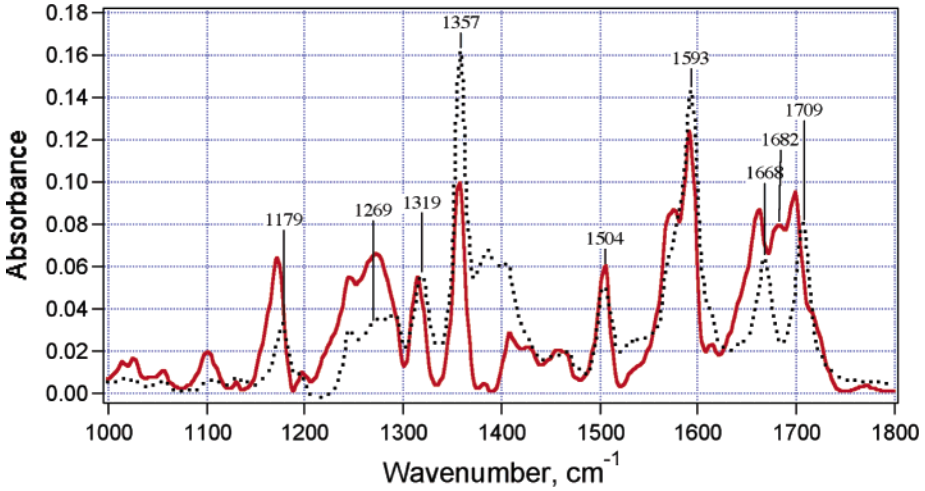

Figure 3. ATR-FTIR spectra of **PMI-T2-TPA** powder (solid line) and mesoscopic TiO_2 film with saturated surface concentration of **PMI-T2-TPA** (dash line).

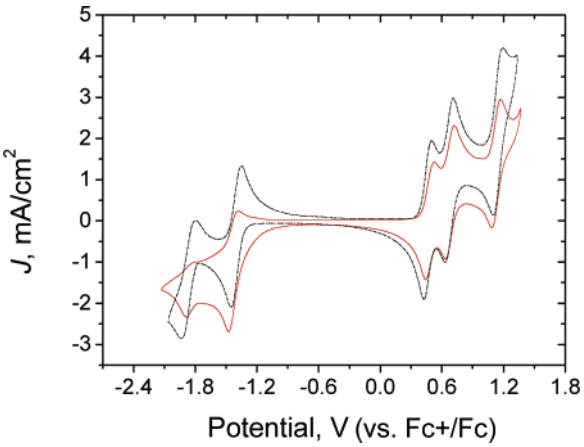

Figure 4. Cyclic voltammogram of 1 mM **PMI-T2-TPA** (solid line) and **3** (dash line) in dichloromethane containing 0.1 M $TBAPF_6$ as supporting electrolyte. The scan rate is 0.1 V/s.

The band at 1680 cm^{-1} assigned to the C═O stretching of the TPA carboxylic acid dimer disappears when adsorbed on mesoscopic TiO_2. Meanwhile, a new band at 1387 cm^{-1} assigned to the carboxylate symmetric —CO_2 stretching appears, but the carboxylate asymmetric —CO_2 stretching at 1620 cm^{-1} is obscured by the 1593 cm^{-1} ring modes. This indicates a strong interaction between the carboxylate group of adsorbed molecules and the substrate.

Electrochemistry of PMI-T2-TPA in Dichloromethane. Shown in Figure 4 are cyclic voltammograms of **PMI-T2-TPA** in CH_2Cl_2 solution. At a scan rate of 0.1 V/s, it shows a reversible one-electron reduction wave at −1.43V ($E_{1/2}$) and a second less reversible reduction wave at −1.87V ($E_{1/2}$). The first one-electron reduction can be assigned to the formation of a radical anion where the major portion of the electron density resides on the carbonyl oxygen due to its electron-withdrawing nature.[26] The second reduction indicates the formation of a radical dianion, possibly from the addition of the second electron to the other carbonyl oxygen of the imide group. It is noted that the irreversibility of this reduction is likely due to the presence of the carboxyl protons as it is reversible for the ester (**3**) in Figure 4. These values agree with the behavior of the parent compound PMI-T2 which exhibits redox waves at −1.42 and −1.87 V ($E_{1/2}$) due to the reduction of the perylene moiety. In the positive potential range three well-pronounced reversible redox waves appear at 0.46, 0.67, and 1.14 V ($E_{1/2}$) indicating the successive formation of stable radical cations, dications, and trications, respectively. We attribute the first two waves to the successive oxidation of the conjugated TPA-T2 unit and the third wave to the independent oxidation of the perylene unit. This assignment is in accordance with the optical spectra and is supported by the electrochemical behavior of the parent compound PMI-T2. In this case the oxidation of the bithiophene part occurs at a distinctly higher potential (i.e., $E_{1/2} = 0.71$ V), and that of the perylene moiety occurs at a slightly lower potential ($E_{1/2} = 1.06$ V).

Electrochemistry of PMI-T2-TPA Monolayer Adsorbed on Nanocrystalline TiO_2 Film. The ionic liquid EMITFSI was chosen for these studies as an electrolyte because **PMI-T2-TPA** is not dissolved in this medium and remains anchored to the mesoscopic oxide films during the electrochemical measurements. Desorption of the triad was observed in polar solvents such as acetonitrile or DMF. Cyclic voltammograms of **PMI-T2-TPA** adsorbed on nanocrystalline TiO_2 film are shown in Figure 5. A reversible 1e reduction wave appears at −1.24 V, and a less reversible reduction at −1.66 V, indicating the formation of a radical anion and the dianion. In addition an irreversible oxidation peak appears at ca. −0.56 V (E_p) probably from a degradation product of the radical dianion. As shown in Figure 6A, when the applied potential is scanned from 0 to −1.50 V in the spectroelectrochemical measurement, a color change from red to dark blue (peak shifts from 520 to 600 nm) is clearly visible. Since the band at 520 nm is due to the $\pi-\pi^*$ charge-transfer transition of perylene, this is consistent with the interpretation of the electrochemical measurements.

The oxidation process of the adsorbed triad on mesoscopic TiO_2 film is much different from that observed in solution. The cyclic voltammogram shows two pairs of waves at 0.79 and 1.28 V for stepwise 1e$^-$ oxidations. Integration of the anodic current associated with the two waves indicates that 80% of the surface adsorbed triad molecules are converted to dication radicals. A sharp irreversible reduction peak appears at around −0.60 V, which arises from the reduction of T2-TPA radical

(26) Lee, S. K.; Zu, Y. B.; Herrmann, A.; Geerts, Y.; Müllen, K.; Bard, A. J. *J. Am. Chem. Soc.* **1999**, *121*, 3513−3520.

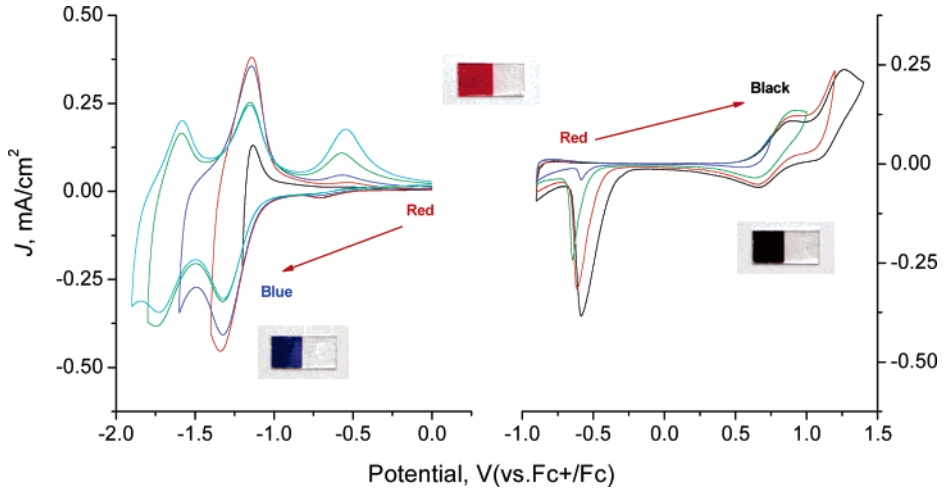

Figure 5. Stepwise cyclic voltammograms of the **PMI-T2-TPA** grafted mesoscopic TiO_2 electrode in EMITFSI. The scan rate is 0.02 V/s. The insets show the color of the film at various applied potentials.

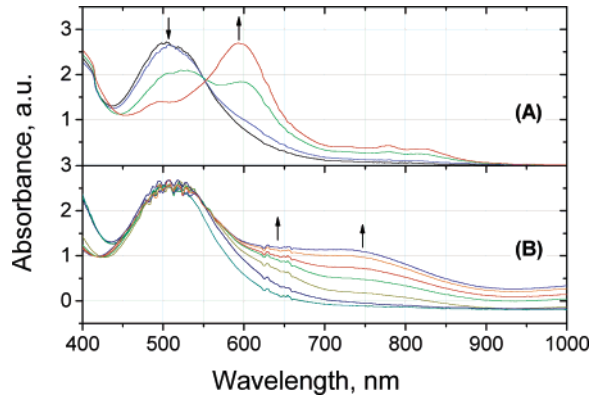

Figure 6. Spectroelectrochemisty of the **PMI-T2-TPA** grafted mesoscopic TiO_2 electrode measured at different potentials. (A) reduction process from 0 to −1.5 V; (B) oxidation process from 0 to 1.5 V.

cation by TiO_2 conduction band electrons, the reduction by cross surface electron-transfer being incomplete.

The **PMI-T2-TPA** derivatized electrode displays striking electrochromism during the oxidation process, a fast color change from red to black being observed as the potential increases from 0 to 1.5 V. During the inverse scan, the color of the electrode does not recover completely unless the applied potential crosses over the irreversible reduction peak at −0.60 V. Spectroelectrochemical measurements are shown in Figure 6B. The first oxidation wave is associated with the appearance of an absorption band around 650 nm, the second one generating a new broad feature at 700 to 800 nm.

These stepwise oxidations can be attributed to the formation of radical cations, the two positive charges being located mainly on the triphenylamine and thiophene moiety, respectively. The absence of any change of the spectral features at 520 nm indicates that the perylene center is not involved in the oxidation within the applied potential range. During the inverse scan, the absorbance between 700 and 800 nm decreases and vanishes when the potential approaches 0 V. Upon passing below −0.6 V, the peak at 650 nm disappears in turn completely and the original **PMI-T2-TPA** absorption spectrum is recovered.

Electrochemistry of PMI-T2-TPA Monolayer Adsorbed on Nanocrystalline Al_2O_3 Film. For comparison, we investigated also the electrochemistry of **PMI-T2-TPA** adsorbed on a mesoscopic Al_2O_3 film, which is insulating in the examined potential range. Figure 7 shows the CVs of the **PMI-T2-TPA** grafted mesoscopic Al_2O_3 electrode at a scan rate of 0.02 V/s. Similar to the nanocrystalline TiO_2 film, one observes chemically reversible waves for the stepwise 1e reduction at −1.22 V and two $1e^-$ oxidations at 0.77 and 1.18 V, respectively. The reduction peak at −0.60 V is absent in the voltammogram in agreement with expectations. As discussed above, the wave at −1.22 V involves formation of a radical anion of the perylene, while the two oxidation waves correspond to the successive injection of positive holes in the triarylamine and thiophene moiety of the triad. The inset of Figure 7 shows the continuous cyclic voltammograms of a triad-grafted mesoscopic Al_2O_3 electrode in the potential range between −1.50 and 1.0 V. Two reversible waves are observed at ca. −1.20 and 0.77 V. After repetitive sweeps, there is practically no change of the CV curves indicating the monolayer remains very stable during prolonged redox cycling. The fraction of triad molecules participating in cross surface electron transfer is around 46% and 18% for oxidation and reduction, respectively.

Similarly to the TiO_2 films, the derivatized Al_2O_3 electrodes also exhibit electrochromism upon varying the potential. However the color reversal is not complete after the second oxidation, the electrode maintaining a blackish tinge during the reverse scan even at potentials as negative as −0.8 V.

Discussion

Nanocrystalline semiconductor films are conductive only in the accumulation regime and are electronically blocking under reverse bias due to the existence of a band gap in the material. Thus, charge-transfer reactions should be restricted to adsorbed species whose redox potential lies above the conduction band edge. For TiO_2 and even more so for Al_2O_3, the flat band potentials are very negative especially in aprotic solvents.[27] It is therefore striking and unexpected to observe the reversible oxidation of **PMI-T2-TPA** grafted on the surface of nanocrystalline TiO_2 or Al_2O_3 films. Three pathways can in principle be invoked to explain the observed electroactivity.[10] They differ in that the electrons are conducted by the semiconductor, transported by molecular diffusion or transferred within the triad monolayer by a hopping process.

(27) Finklea, H. O. *Semiconductor Electrodes;* Elsevier: Amsterdam, 1988; pp 108−114.

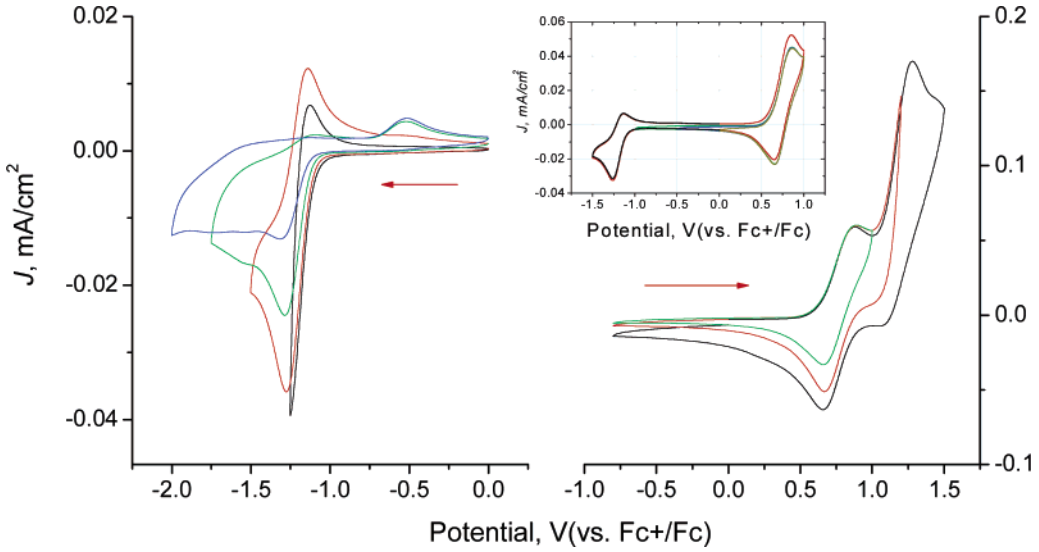

Figure 7. Stepwise cyclic voltammograms of the **PMI-T2-TPA** grafted mesoscopic Al_2O_3 electrode in EMITFSI. The inset shows the continuous cyclic voltammograms of **PMI-T2-TPA** derivatized mesoscopic Al_2O_3 electrode between −1.50 and 1.0 V. The scan rate is 0.02 V/s.

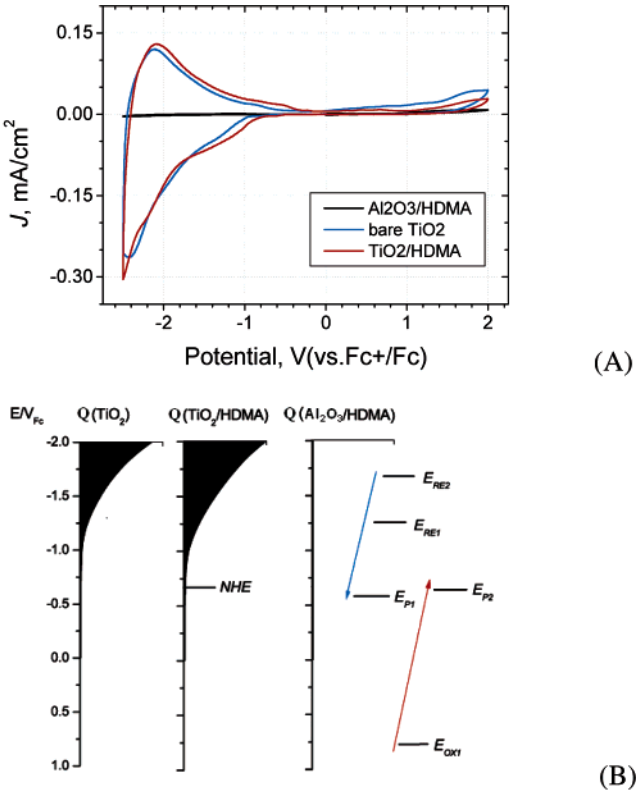

Figure 8. (A) Cyclic voltammograms of bare and HDMA grafted oxide electrodes in EMITFSI. (Black line) HDMA grafted Al_2O_3; (blue line) bare TiO_2; (red line) HDMA grafted TiO_2. The scan rate is 0.02 V/s. (B) Energy levels at mesoscopic metal oxides (HDMA grafted nanocrystalline TiO_2 and Al_2O_3)/ EMITFSI interface. E_{RE} and E_{OX} are the formal potentials of **PMI-T2-TPA** on TiO_2; E_P is the relevant peak potential.

The first hypothesis implies that an electron flow either in the conduction band of the semiconductor or in trap states along its surface. The latter mechanism requires the density of available surface states to be sufficiently high to support the charge hopping. Forward bias of the TiO_2 layer in contact with the EMITFSI ionic liquid resulted in a capacitive current shown in the Figure 8A. Cyclic voltammograms of films in the bare state and grafted with the electrochemically inert amphiphilic HDMA molecules were measured. For an ideal n-type semiconductor, charge injection should be turned on once the Fermi level reaches the conduction band edge. The gradual onset of the capacitive current in Figure 8A indicates that a tail of surface states exists below the bulk conduction band edge probably due to the presence of coordinatively unsaturated Ti^{4+} ions on the surface of the TiO_2 nanoparticles.[28,29] The wave during the reverse scan shows a nearly complete recovery of the injected negative charge, indicating that most surface states are emptied on the cyclic voltammetric time scale.

The energetic distribution of acceptor states at the surface of the mesoscopic TiO_2 electrode can be derived directly from the cyclic voltammograms, since the current $I(V)$ is proportional to the differential capacity (C) in a linear sweep (constant scan rate, $dV/dt = \nu$).

$$dQ = \frac{1}{\nu} I(V)\, dV \tag{3}$$

Dividing the derivative dQ/dV by elementary charge yields the density of occupied states (DOS), whereas the total injected charge (Q) can be obtained by integration of eq 3. The latter is plotted in Figure 8B as a function of the electrode potential. The onset for bare TiO_2 is around −1.0 V, whereas it is shifted positively to −0.75 V for HDMA grafted films due to surface protonation by the carboxylic acid group.[30,31] In both cases, the number of surface states is very small at positive voltages. As expected, the Al_2O_3 electrode showed insulating behavior over the whole investigated potential range.

It is clear from these results that the reduction of **PMI-T2-TPA** molecules grafted on the mesoscopic TiO_2 film can be carried out by electrons that are injected from the FTO glass electrode into the semiconductor particles and migrate in the conduction band of the oxide or via surface states to be finally transferred to the perylene acceptor. By contrast, the successive

(28) Hagfeldt, A.; Grätzel, M. *Chem. Rev.* **1995**, *95*, 49−68.
(29) Moser, J.; Punchihewa, S.; Infelta, P. P.; Grätzel, M. *Langmuir* **1991**, *7*, 3012−3018.
(30) Lantz, J. M.; Baba, R.; Corn, R. M. *J. Phys. Chem.* **1993**, *97*, 7392−7395.
(31) Nelson, B. P.; Candal, R.; Corn, R. M.; Anderson, M. A. *Langmuir* **2000**, *16*, 6094−6101.

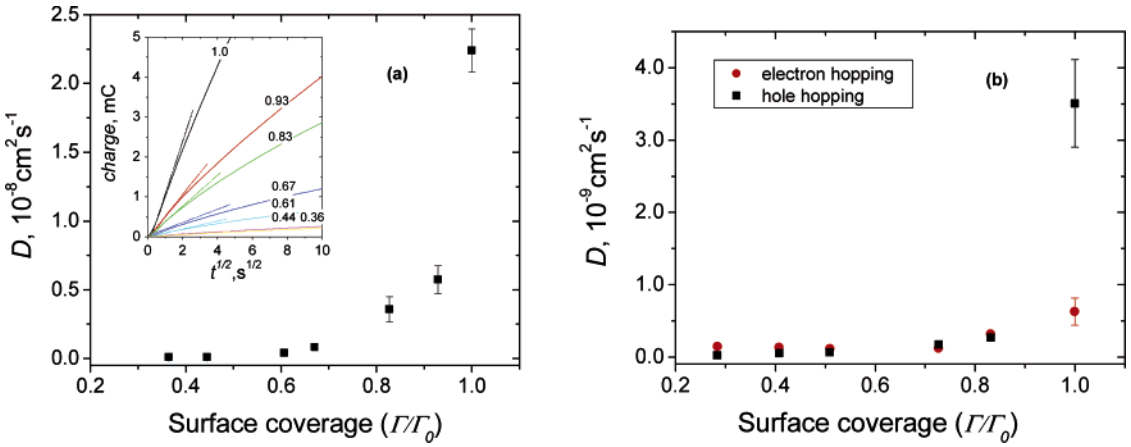

Figure 9. D_{app} of charge hopping in monolayer of **PMI-T2-TPA** assembled on TiO_2 (a) and Al_2O_3 (b) as a function of Γ/Γ_0. The square dots show the hole hopping rates upon polarizing the **PMI-T2-TPA** derivatized TiO_2 (a) or Al_2O_3 (b) electrodes to 1.0 V vs Fc+/Fc (see the Cottrell plots in the inset of part a determined by chronocoulometry with polarization potential of 1.0 V. The marked values indicate different surface coverages). The circle dots in part b show the electron hopping rates upon polarizing the derivatized Al_2O_3 electrodes to −1.5 V.

two-electron oxidation of the triad grafted on TiO_2 and the redox processes observed on nanocrystalline Al_2O_3 electrode must occur via a different mechanism.

One plausible hypothesis is that the **PMI-T2-TPA** molecules are sufficiently mobile inside the monolayer or undergo a dynamic exchange between the surface and the contacting solution, to be able to transport electrons by diffusion to the underlying conducting glass. Such a mechanism explains the electroactivity of amphiphilic viologens adsorbed on mesoporous Al_2O_3 films.[32−34] However, if the anchoring of the molecules to the metal oxide surface is strong enough to prevent any significant diffusion, charge transport can only take place by electron hopping between molecules inside the monolayer. Diffusive and hopping charge transport exhibit very different behaviors. When the two mechanisms are operative in parallel, the apparent diffusion coefficient can be expressed as[35]

$$D_{app} = D_{phy} + k_{ex}\delta^2 c/6 \qquad (4)$$

Here D_{phy} reflects the contribution from physical diffusion while the second term, derived by Dahms−Ruff (DR)[36,37] and Laviron−Andrieux−Savéant (LAS)[38−41] equation, describes the electron hopping process, k_{ex} being the self-exchange rate constant, δ being the intermolecular distance at which the electron transfer takes place, and c being the concentration of electroactive species. If the molecular motion prevails, the diffusion coefficient should be independent of the concentration. On the contrary, if charges are transported by electron hopping, D_{app} increases with the concentration of the electroactive species and there is a percolation threshold, below which no conduction is observed.

To discriminate these two processes, the apparent diffusion coefficient D_{app} was determined by chronocoulometry at different **PMI-T2-TPA** surface concentrations, coadsorbed HDMA molecules being employed as inert diluents. The potential of the nanocrystalline TiO_2 film was stepped from 0 to 1.0 V, and the charge−time profiles were recorded. The data are plotted in Figure 9a together with the apparent diffusion coefficients derived from the Cottrell equation:

$$Q = 2nFSc\sqrt{\frac{D_{app}t}{\pi}} \qquad (5)$$

The results demonstrate that the degree of coverage of the mesoscopic TiO_2 surface by **PMI-T2-TPA** has a dramatic effect on D_{app}. In agreement with the theoretical predictions for two-dimensional charge percolation,[42] hole injection is only observed above a threshold concentration where the triad occupies ca. 50% of the TiO_2 surface. Above this threshold the diffusion coefficient increases sharply with the concentration of **PMI-T2-TPA** confirming a charge hopping mechanism to be operative. The holes are injected from the exposed conducting glass support into the T2-TPA unit from where they are transported across the surface by an exchange process. Similarly, the second oxidation of **PMI-T2-TPA** grafted on TiO_2 at around 1.28 V can be presumed to happen through lateral charge transfer between adjacent T2-TPA centers. The appearance of a percolation threshold indicates that the Faradic currents observed with the **PMI-T2-TPA** covered insulating oxides arise from cross surface charge hopping and not from the surface diffusion of the adsorbate. Hence the D_{phys} in eq 4 can be neglected with respect to the exchange term.

At full loading of **PMI-T2-TPA** on TiO_2, the self-exchange rate constant k_{ex} is calculated to be 2.0×10^7 M^{-1} s^{-1}, using the value $D_{app} = 2.2 \times 10^{-8}$ cm^2 s^{-1}, $\delta = 1.2$ nm and $c = 0.47$ M from the isotherm measurements and molecular model-

(32) Miller, C. J.; Majda, M. *J. Am. Chem. Soc.* **1986**, *108*, 3118−3120.
(33) Miller, C. J.; Majda, M. *J. Electrochem. Soc.* **1986**, *133*, C128.
(34) Miller, C. J.; Widrig, C. A.; Charych, D. H.; Majda, M. *J. Phys. Chem.* **1988**, *92*, 1928−1936.
(35) Leone, A. M.; Weatherly, S. C.; Williams, M. E.; Thorp, H. H.; Murray, R. W. *J. Am. Chem. Soc.* **2001**, *123*, 218−222.
(36) Dahms, H. *J. Phys. Chem.* **1968**, *72*, 362−364.
(37) Ruff, I.; Friedric, V. J.; Csillag, K. *J. Phys. Chem.* **1972**, *76*, 162−165.
(38) Laviron, E. *J. Electroanal. Chem.* **1980**, *112*, 1−9.
(39) Laviron, E.; Roullier, L.; Degrand, C. *J. Electroanal. Chem.* **1980**, *112*, 11−23.
(40) Andrieux, C. P.; Saveant, J. M. *J. Electroanal. Chem.* **1980**, *111*, 377−381.
(41) Anson, F. C.; Blauch, D. N.; Saveant, J. M.; Shu, C. F. *J. Am. Chem. Soc.* **1991**, *113*, 1922−1932.
(42) Sahimi, M. *Application of Percolation Theory;* Taylor & Francis: London, 1994; pp 1−22.

(43) The self-exchange rate constant k_{ex} was calculated according to the equation $k_{ex} = 6D_{app}/(\delta^2 c)$. D_{app} was obtained from a Cottrell plot. $\delta = 2\sqrt{A^*/\pi}$, where A^*, the area occupied by one **PMI-T2-TPA** molecule on the TiO_2 surface, was obtained from the isotherm measurements. $c = \Gamma^\circ/d$ is the volume concentration contained within the molecular monolayer, where the thickness d of the monolayer was derived from molecular modeling to be ~3.1 nm.

ing.[43] The diffusion-limited rate constant k_d in 1-butyl-3-methylimidazolium bis(trifluoromethanesulfonyl)amide ionic liquid, which has higher viscosity than EMITFSI, is reported to be 3.8×10^8 M^{-1} s^{-1}.[44,45] Thus, k_{ex} is 1 order of magnitude lower than k_d, indicating the surface charge percolation is limited by the self-exchange rate rather than charge compensation from electrolyte.

The fact that the oxidation of **PMI-T2-TPA** is accompanied by the insertion of anions (e.g., $TFSI^-$) to counterbalance the positive charge of the cation radicals separates the adjacent triad molecule interrupting the percolation pathway.[12] This is probably the reason for the poor reversibility of the second oxidation. During the return scan, cation radicals are reduced to the original state of the triad by cross surface electron transfer. Electron percolation is hampered by the intercalation of TFSI anions between the positively charged **PMI-T2-TPA** relay molecules, isolating a significant fraction of the triad molecules. These will remain in the oxidized state until at -0.60 V the conduction pathway of electrons via TiO_2 surface states is turned on making them accessible to reduction.

Figure 5 shows that the charge associated with the cathodic peak at -0.6 V augments markedly by increasing the positive limit of the electrode potential applied during the oxidation process. If only the first oxidation of the triad is carried out, this charge becomes very small suggesting that the reduction concerns mainly residual radical cations arising from the second oxidation of T2-TPA unit. This is plausible, since the presence of two positive charges will enhance the intercalation of TFSI anions between adjacent **PMI-T2-TPA** blocking the percolation channel. Our spectroelectrochemical results indicate that the first anodic wave corresponds to oxidation of the TPA unit and the second corresponds to that of the T2 moiety. It is the latter oxidation that appears to induce significant TFSI anion insertion in the film, interrupting cross surface charge migration.

Since the cross surface hole percolation within a molecular monolayer accompanies simultaneous charge compensation from an electrolyte, one would expect a faster hopping rate by using low viscosity solvent[10] or increasing the concentration of anion. This was confirmed to be the case also for the **PMI-T2-TPA** monolayer. Thus in dimethyl carbonate solvent, the **PMI-T2-TPA** oxidation and reduction currents increased with the ionic strength of the electrolyte. However the use of these solvents poses stability problems as the triad was found to desorb from the oxide surface under continuous cycling of the electrode potential. A much more stable performance was reached with the ionic liquid electrolyte.

Because the mesoscopic Al_2O_3 film is insulating in the investigated potential range between -2.5 to $+2$ V, the appearance of the reversible reduction and oxidation waves clearly indicates the occurrence of lateral electron hopping within the self-assembled **PMI-T2-TPA** monolayer. The cross surface charge transfer is initiated by electron and hole injection from the FTO electrode support into the electroactive monolayer. Note the absence of a surface state mediated reduction of the **PMI-T2-TPA** cation radicals conferring a persistent blackish color to the film after oxidation.

Figure 9b depicts the dependence of the apparent diffusion coefficient of charge hopping on surface coverage of **PMI-T2-TPA** adsorbed on Al_2O_3 upon polarizing the mesoscopic electrode to -1.50 and 1.0 V. A similar threshold at around 70% surface coverage is observed for both hole and electron hopping. The hole hopping is about 5.5 times faster than the electron hopping for the pure **PMI-T2-TPA** monolayer. Note that the diffusion coefficient for cross surface hole transfer is 6 times lower for the mesoscopic Al_2O_3 as compared to the TiO_2 film, which is in keeping with the smaller yield of cross surface charge transfer observed for the former electrodes. These differences are thought to reflect the quality of the morphology of the mesoscopic film and that of the adsorbed **PMI-T2-TPA** monolayer.

Conclusions

Cross surface ambipolar charge percolation was witnessed within a monolayer of a molecular triad adsorbed on insulating mesoscopic Al_2O_3 films. The triad consists of a triphenlyamine (TPA) donor and a perylenemonoimide (PMI) acceptor connected by a bithiophene (T2) bridge. The self-assembled **PMI-T2-TPA** monolayer exhibits p-type or n-type conduction depending on the potential that is applied to the FTO electrode supporting the oxide films. Cross surface electrons transfer is turned on at negative polarization where the PMI moiety is electroactive. The color of the film changes from red to blue during the reduction of the PMI. By contrast, lateral hole transfer is turned on at positive polarization where the TPA moiety becomes electroactive. The stepwise oxidation of the T2-TPA units is associated with a color change of the film from red to black. It is associated with the intercalation of anions in the monomolecular film. An intriguing observation is that this insertion blocks at least partially the cross surface charge transfer. Cyclic voltammetric as well as chronocoulometric and spectroelectrochemical measurements were applied to determine the percolation threshold for cross surface charge transfer and the diffusion coefficients for the electron and hole hopping process. On nanocrystalline TiO_2 films, an additional pathway of electron transport in the conduction band of the oxide or via surface states becomes available under forward bias which allows the reduction of triad cation radicals that have become inaccessible to cross surface charge transfer as a result of the anion intercalation process. Our observations open up a realm of new opportunities in molecular electronics and the design of novel information storage and electrochromic systems.

Acknowledgment. We acknowledge financial support of this work by the Swiss Science Foundation under National Program No. 47 and COST D14 Action Program of the European Community. J. Cremer thanks the "Fonds der Chemischen Industrie" and the German Ministry of Education and Research (BMBF) for a Kekulé-Grant. We thank Mr. P. Comte and R. Charvet for providing mesoscopic metal oxide films.

Supporting Information Available: Synthesis and characterization data of **PMI-T2-TPA**. This material is available free of charge via the Internet at http://pubs.acs.org.

JA0426701

(44) Gordon, C. M.; McLean, A. J. *Chem. Commun.* **2000**, 1395−1396.
(45) McLean, A. J.; Muldoon, M. J.; Gordon, C. M.; Dunkin, I. R. *Chem. Commun.* **2002**, 1880−1881.